ethane increases linearly with the number of methyl groups in Cp′ (N_{Me}) from C_5H_5 to C_5Me_5. For each methyl group ΔH_{HM} changes by −1.1 kcal mol^{-1} ($\delta\Delta H_{HM}$). The ΔH_{HM} values correlate with the chemical shift of the olefin ^{1}H NMR resonance in the 1,5-COD ligand of the neutral complexes and the Ir-H ^{1}H NMR resonance of the protonated products.

Equilibrium studies of the proton transfer reactions (eq 3) show that the successive addition of methyl groups to the Cp′ ring changes $\Delta G^{\ominus}$ by −0.89 ± 0.06 kcal mol^{-1} per methyl group and $\Delta S^{\ominus}$ by −0.7 ± 0.7 eu per methyl. Thus, the differences in basicities (K_{eq} or $\Delta G^{\ominus}$) of the various methyl-substituted Cp′Ir(1,5-COD) complexes are largely determined by ΔH_{HM} values of the complexes, and $\Delta S^{\ominus}$ makes a relatively small contribution. Comparing the common C_5H_5 and C_5Me_5 ligands, one finds that replacing C_5H_5 in (C_5H_5)Ir(1,5-COD) by C_5Me_5 increases the equilibrium constant, K_{eq}, for the protonation of the complex by 1900; $\Delta G^{\ominus}$ becomes more favorable by −4.5 kcal mol^{-1}; ΔH_{HM} becomes more favorable by −5.7 kcal mol^{-1}, while $\Delta S^{\ominus}$ becomes slightly less favorable by ∼−4 eu.

Acknowledgment. We thank the National Science Foundation (Grant CHE-8719744) for their support of this research. The loan of $IrCl_3 \cdot xH_2O$ from Johnson Matthey is greatly appreciated. We are also grateful to Dr. Vinko Rutar and Dr. Dave Scott of the Iowa State University Chemical Instrument Services for their assistance with the NMR experiments.

Reactions of Cp*Ir(2,5-dimethylthiophene) with Iron Carbonyls: A New Mechanism for Thiophene Hydrodesulfurization

Jiabi Chen, Lee M. Daniels,[†] and Robert J. Angelici*

Contribution from Ames Laboratory[1] and the Department of Chemistry, Iowa State University, Ames, Iowa 50011. *Received September 4, 1990*

Abstract: Reactions of the isomers Cp*Ir(η^4-2,5-Me_2T) (**1**) and Cp*Ir(*C,S*-2,5-Me_2T) (**2**), where Cp* = η^5-C_5Me_5 and 2,5-Me_2T = 2,5-dimethylthiophene, with iron carbonyls ($Fe(CO)_5$, $Fe_2(CO)_9$, and $Fe_3(CO)_{12}$) give eight different products, **3**–**10**. Two of them, Cp*Ir(η^4-2,5-Me_2T·$Fe(CO)_4$) (**3**) and Cp*Ir(η^4-2,5-Me_2T·$Fe_2(CO)_7$) (**7**), retain the η^4-2,5-Me_2T coordination to the Ir but are also bonded through the sulfur to the Fe atom(s). Both **1** and **2** react with $Fe_3(CO)_{12}$ to give **8** in which all of the elements of 2,5-Me_2T are present but the sulfur has been removed from the thiophene ring. Reaction of **8** with CO (1 atm)

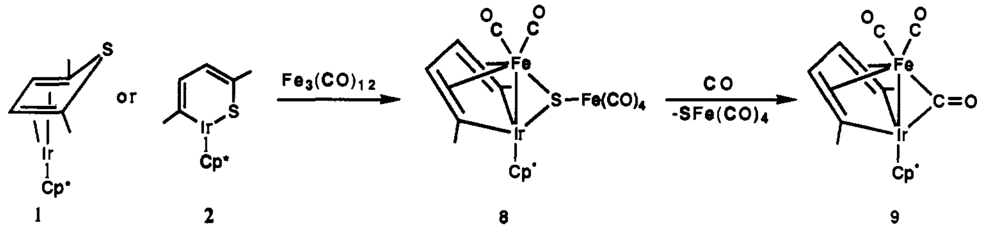

1 **2** **8** **9**

gives the totally desulfurized **9**. A new mechanism is proposed for thiophene hydrodesulfurization (HDS) based on the C–S bond cleavage reactions which occur when **1** rearranges to **2** and **2** is converted to **8**. Structures of **3**, **7**, **8**, and **9** were established by X-ray diffraction studies.

On the basis of organometallic model compound and catalytic reactor studies, a mechanism (Scheme I) was proposed[2,3] in these laboratories for the transition-metal-catalyzed hydrodesulfurization (HDS) of thiophene to give H_2S and C_4 hydrocarbons. The actual desulfurization step (Scheme I), which involves C–S bond cleavage, occurs after thiophene is partially hydrogenated to dihydrothiophene. Very recently[4] we observed another type of C–S bond cleavage (eq 1) in thiophene itself. In this base-catalyzed rearrangement, the iridium in Cp*Ir(η^4-2,5-Me_2T) (**1**) inserts into a C–S bond of the η^4-thiophene to give the ring-opened iridathiabenzene Cp*Ir(*C,S*-2,5-Me_2T)[5] (**2**), where Cp* is η^5-C_5Me_5 and

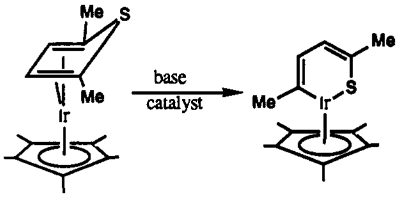

(1)

1 **2**

Scheme I. Hydrogenation Mechanism for Thiophene HDS[2,3]

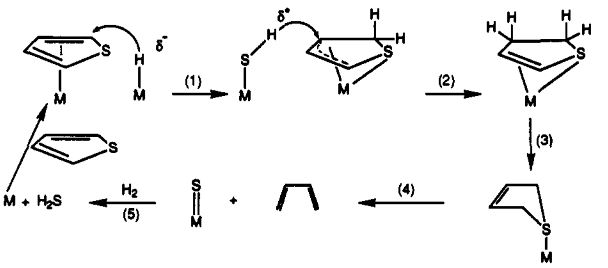

[†] Iowa State University Molecular Structure Laboratory.

[1] Ames Laboratory is operated by the U.S. Department of Energy by Iowa State University under Contract W-7405-Eng-82. This research was supported by the Office of Basic Energy Sciences, Chemical Sciences Division.

[2] (a) Sauer, N. N.; Markel, E. J.; Schrader, G. L.; Angelici, R. J. *J. Catal.* **1989**, *117*, 295. (b) Markel, E. J.; Schrader, G. L.; Sauer, N. N.; Angelici, R. J. *J. Catal.* **1989**, *116*, 11.

0002-7863/91/1513-2544$02.50/0

2,5-Me_2T is 2,5-dimethylthiophene. Both **1** and **2** undergo a variety of reactions. With the Lewis acids BH_3 and $Cp(CO)_2Mo{\equiv}Mo(CO)_2Cp$, they form the sulfur adducts Cp*Ir(η^4-2,5-$Me_2T{\cdot}BH_3$)[4,6,7] and Cp*Ir(η^4,*S*-μ_3-2,5-Me_2T)[$Mo(CO)_2Cp]_2$.[8] With Lewis bases (L) such as phosphines and CO, **1** and **2** react to form metal adducts of the ring-opened thiophene Cp*Ir(*C*,*S*-2,5-Me_2T)(L).[9] They also form the ring-opened thiophene dihydride complex Cp*Ir(*C*,*S*-2,5-Me_2T)$(H)_2$ upon reaction with H_2.[9]

The C–S bond cleavage in eq 1 could lead one to conceive of this as a first step in a new HDS mechanism in which C–S cleavage occurs prior to hydrogenation of the thiophene. On a heterogeneous HDS catalyst, it is likely that there will be other metal atoms adjacent to the one at which thiophene adsorption and ring-opening of the type in eq 1 might occur. Thus, in this report we explore the reactions which occur when iron carbonyl complexes ($Fe(CO)_5$, $Fe_2(CO)_9$, and $Fe_3(CO)_{12}$) are added to **1** and **2**. The results suggest a pathway for the complete desulfurization of **2** and a new mechanism for catalytic thiophene HDS.

Experimental Section

General Procedure. All reactions were performed in an N_2 atmosphere following standard Schlenk techniques. All solvents employed were reagent grade and dried by refluxing over appropriate drying agents and stored over 4-Å molecular sieves under an N_2 atmosphere until use. Tetrahydrofuran (THF) and diethyl ether (Et_2O) were distilled from potassium benzophenone ketyl, while hexane and CH_2Cl_2 were distilled from CaH_2. The neutral Al_2O_3 (Brockmann, Activity I, 80–100 mesh) used for chromatography was deoxygenated under high vacuum at room temperature for 16 h, deactivated with 5% (w/w) N_2-saturated water, and stored under N_2; columns were 1.5 × 10–20 cm. The $Fe(CO)_5$ and $Fe_2(CO)_9$, were purchased from Strem Chemicals, Inc. and Pressure Chemical Co., respectively. The gases CO and H_2 were used as purchased. The complexes Cp*Ir(η^4-2,5-Me_2T) (**1**), Cp*Ir(*C*,*S*-2,5-Me_2T) (**2**), and [Cp*Ir(η^5-2,5-Me_2T)]$(BF_4)_2$ (**11**) were prepared as previously described.[3,4] The $Fe_3(CO)_{12}$,[10] $(NEt_4)_2Fe_2(CO)_8$,[11] and $Cp_2Fe(PF_6)$[12] were prepared by literature methods. All elemental analyses were performed by Galbraith Laboratory, Inc. The IR spectra were measured on a Perkin-Elmer 681 spectrophotometer. All ^1H NMR spectra were recorded at ambient temperature in $CDCl_3$ or CD_3NO_2 solution with $CHCl_3$ or CHD_2NO_2 as the internal reference using a Nicolet NT-300 spectrometer. Electron ionization mass spectra (EIMS) were run on a Finnigan 4000 spectrometer. Fast atom bombardment (FAB) spectra were run on a Kratos MS-50 mass spectrometer with a 3-nitrobenzyl alcohol/CH_3NO_2 matrix. Melting points were recorded in sealed nitrogen-filled capillaries and are uncorrected.

Reaction of Cp*Ir(η^4-2,5-Me_2T) (1) with $Fe(CO)_5$ To Give Cp*Ir(η^4-2,5-$Me_2T{\cdot}Fe(CO)_4$) (3) and Cp*Ir(2,5-Me_2T)($Fe(CO)_4$) (4). To 40 mg (0.091 mmol) of **1** dissolved in 30 mL of THF at 0 °C was added 26 mg (0.133 mmol) of $Fe(CO)_5$. The mixture was stirred at 0–15 °C for 3 h during which time the light yellow solution gradually turned orange-red. After evaporating the solution under vacuum to dryness, the residue was chromatographed on Al_2O_3 (neutral) with hexane/CH_2Cl_2 (20:1) as the eluant. The yellow band which eluted first was collected and then the orange band was eluted with hexane/CH_2Cl_2 (10:1). After vacuum removal of the solvents from the above two eluates, the residues were recrystallized from hexane/CH_2Cl_2 at −80 °C. From the first fraction, 14 mg (25%, based on **1**) of yellow crystals of **3** were obtained (mp 162–164 °C dec). IR (hexane) ν_{CO}: 2038 vs, 1958 s, 1929 vs, br cm^{-1}. ^1H NMR ($CDCl_3$): δ 4.54 (s, 2 H), 1.94 (s, 15 H), 1.35 (s, 6 H). MS: *m/e* 608 (M^+), 552 (M^+ − 2CO), 524 (M^+ − 3CO), 496 (M^+ − 4CO), 440 (M^+ − $Fe(CO)_4$). Anal. Calcd for $C_{20}H_{23}O_4SIrFe$: C, 39.54, H, 3.82. Found: C, 39.30; H, 3.80. From the second fraction, 6 mg (11%) of **4** as orange-red crystals were obtained (mp 182–184 °C dec). IR (hexane) ν_{CO}: 2035 vs, 1952 s, 1924 vs, br cm^{-1}. ^1H NMR ($CDCl_3$): δ 7.70 (d, 1 H), 7.52 (d, 1 H), 2.27 (s, 3 H), 2.03 (s, 3 H), 1.86 (s, 15 H). MS: *m/e* 608 (M^+), 580 (M^+ − CO), 552, (M^+ − 2CO), 524 (M^+ − 3CO), 496 (M^+ − 4CO), 440 (M^+ − $Fe(CO)_4$). Anal. Calcd for $C_{20}H_{23}O_4SIrFe$: C, 39.54; H, 3.82. Found: C, 39.60; H, 3.78.

Reaction of Cp*Ir(*C*,*S*-2,5-Me_2T) (2) with $Fe(CO)_5$ To Give Cp*Ir(*C*,*S*-2,5-Me_2T)(CO) (5). A solution of **2** (25 mg, 0.057 mmol) in THF (20 mL) was treated with $Fe(CO)_5$ (25 mg, 0.128 mmol) at 0–15 °C for 3 h during which time the red solution turned orange gradually. The resulting mixture was evaporated under vacuum to dryness. The residue was chromatographed on Al_2O_3 (neutral) with hexane/CH_2Cl_2 (20:1) as the eluant, and the yellow band was collected. After vacuum removal of the solvent, the crude orange powder product was recrystallized from hexane at −80 °C to give 6 mg (22%, based on **2**) of orange-yellow needles of **5** (mp 121 °C dec). IR (hexane) ν_{CO}: 2020 s cm^{-1}. ^1H NMR ($CDCl_3$): δ 5.73 (d, 1 H), 5.40 (d, 1 H), 2.24 (s, 3 H), 1.92 (s, 3 H), 1.85 (s, 15 H). MS: *m/e* 468 (M^+), 440 (M^+ − CO), 356 (M^+ − Me_2T). Anal. Calcd for $C_{17}H_{23}OSIr$: C, 43.66; H, 4.96. Found: C, 44.06; H, 5.28.

Reaction of 1 with $Fe_2(CO)_9$ To Give Cp*Ir(η^4-2,5-$Me_2T{\cdot}Fe(CO)_4$) (3), Cp*Ir(2,5-Me_2T)$Fe_2(CO)_8$ (6), and Cp*Ir(η^4-2,5-$Me_2T{\cdot}Fe_2(CO)_7$) (7). To a stirred, light yellow solution of **1** (42 mg, 0.096 mmol) in THF (40 mL) at approximately −10 °C was added 50 mg (0.137 mmol) of $Fe_2(CO)_9$. Immediately the solution became orange-red in color. After the reaction solution was permitted to warm slowly to 0 °C, it was stirred for 3 h at 0–15 °C. The solvent was then removed under vacuum to obtain a dark purple residue. This residue was chromatographed on Al_2O_3 (neutral) with hexane as the eluant. The purple-red band which eluted first was collected and then a yellow band was eluted with hexane/CH_2Cl_2 (15:1) and collected. A third band (green-yellow) was eluted with hexane/CH_2Cl_2/Et_2O (10:1:1). After vacuum removal of the solvents from the above three eluates, the residues were recrystallized from hexane or hexane/CH_2Cl_2 at −80 °C. From the first fraction, 18 mg (24%, based on **1**) of purple-red crystals of **6** were obtained (mp 142–143 °C dec). IR (hexane) ν_{CO}: 2008 vs, 1957 vs, 1948 s, 1720 vs, br cm^{-1}. ^1H NMR ($CDCl_3$): δ 5.59 (d, 1 H), 3.61 (d, 1 H), 2.43 (s, 3 H), 2.04 (s, 15 H), 1.85 (s, 3 H). MS: *m/e* 776 (M^+), 748 (M^+ − CO), 720 (M^+ − 2CO), 664 (M^+ − 4CO), 608 (M^+ − 6CO), 552 (M^+ − 8CO). Anal. Calcd for $C_{24}H_{23}O_8SIrFe_2$: C, 37.14; H, 3.00. Found: C, 37.08, H, 3.31. From the second fraction, 16 mg (28%) of **3** as yellow crystals were obtained (mp 162–164 °C dec). IR (hexane) ν_{CO}: 2038 vs, 1958 s, 1929 vs, br cm^{-1}. ^1H NMR ($CDCl_3$): δ 4.54 (s, 2 H), 1.94 (s, 15 H), 1.35 (s, 6 H). From the third fraction, 22 mg (31%) of **7** as dark-green crystals were obtained (mp 117–118 °C dec). IR (CH_2Cl_2) ν_{CO}: 2041 vs, 1998 vs, 1952 vs, br, 1750 s, br cm^{-1}. ^1H NMR ($CDCl_3$): δ 4.80 (s, 2 H), 1.97 (s, 15 H), 1.24 (s, 6 H). MS: *m/e* 748 (M^+), 720 (M^+ − CO), 692 (M^+ − 2CO), 664 (M^+ − 3CO), 636 (M^+ − 4CO), 580 (M^+ − 6CO), 552 (M^+ − 7CO), 440 (M^+ − $Fe_2(CO)_7$). Anal. Calcd for $C_{23}H_{23}O_7SIrFe_2$: C, 36.96; H, 3.10. Found: C, 36.84; H, 3.28.

Reaction of 2 with $Fe_2(CO)_9$ To Give 3, 6, Cp*Ir(C(Me)=CHCH=C(Me))[μ-SFe(CO)$_4$]Fe(CO)$_2$ (8), and Cp*Ir(C(Me)=CHCH=C(Me))(μ-CO)Fe(CO)$_2$ (9). Similar to the procedures described above for the reaction of **1** with $Fe_2(CO)_9$, a stirred red solution of **2** (55 mg, 0.125 mmol) in THF (40 mL) at approximately −10 °C was treated with $Fe_2(CO)_9$ (70 mg, 0.192 mmol). The solution was stirred at 0–15 °C for 3 h during which time the red solution turned dark purple gradually. After vacuum removal of the solvent, the residue was chromatographed on Al_2O_3 (neutral) with hexane as the eluant. A purple-red band which eluted first was collected and then an orange band was eluted with hexane/CH_2Cl_2 (20:1). A third band (yellow) was eluted with hexane/CH_2Cl_2 (10:1), and a fourth dark-purple band was eluted with hexane/CH_2Cl_2/Et_2O (10:1:1). Further treatment of the above four eluates as described above for the reaction of **1** with $Fe_2(CO)_9$ gave 26 mg (27%, based on **2**) of purple-red crystals of **6**, 14 mg (21%) of orange-red crystals of **9**, 17 mg (22%) of yellow crystals of **3**, and 23 mg (26%) of **8** as dark blue-purple crystals. **6**: mp 143 °C dec. IR (hexane) ν_{CO}: 2008 vs, 1958 vs, 1948 s, 1720 vs, br cm^{-1}. ^1H NMR ($CDCl_3$): δ 5.59 (d, 1 H), 3.61 (d, 1 H), 2.43 (s, 3 H), 2.04 (s, 15 H), 1.85 (s, 3 H). **9**: mp 178–179 °C dec. IR (hexane) ν_{CO}: 2000 vs, 1948 vs, 1842 s cm^{-1}. ^1H NMR ($CDCl_3$): δ 5.77 (s, 2 H), 2.22 (s, 6 H), 1.90 (s, 15 H). MS: *m/e* 548 (M^+), 520 (M^+ − CO), 492 (M^+ − 2CO), 464 (M^+ − 3CO), 408 (M^+ − $Fe(CO)_3$). Anal. Calcd for $C_{19}H_{23}O_3IrFe$: C, 41.69; H, 4.23. Found: C, 41.79; H, 4.31. **3**: mp 163 °C dec. IR (hexane) ν_{CO}: 2038 vs, 1958 s, 1928 vs, br cm^{-1}. ^1H NMR ($CDCl_3$): δ 4.54 (s, 2 H), 1.94 (s, 15 H), 1.35 (s, 6 H). **8**: mp 140–141 °C dec. IR (CH_2Cl_2) ν_{CO}: 2040 vs, 2000 s, 1963 m, br, 1920 s, br cm^{-1}. ^1H NMR ($CDCl_3$): δ 5.68 (s, br, 1 H), 5.35 (s, br, 1 H), 2.74 (s, 3 H), 2.07 (s, 3 H), 1.79 (s, 15 H). MS: *m/e* 664 (M^+ − 2CO), 636 (M^+ − 3CO), 580 (M^+ − 5CO),

---

[3] Angelici, R. J. *Acc. Chem. Res.* **1988**, *21*, 387.

[4] Chen, J.; Daniels, L. M.; Angelici, R. J. *J. Am. Chem. Soc.* **1990**, *112*, 199.

[5] Previously[3,4] the *C*,*S*-2,5-Me_2T ligand in this complex was abbreviated η^2-2,5-Me_2T. This change is made in order to avoid confusion with a 2,3-η^2-thiophene ligand proposed recently for $(NH_3)_5Os(2,3\text{-}\eta^2\text{-thiophene})^{2+}$ (Cardone, R.; Harman, W. D.; Taube, H. *J. Am. Chem. Soc.* **1989**, *111*, 5969).

[6] Chen, J.; Angelici, R. J. *Organometallics* **1989**, *8*, 2277.

[7] Chen, J.; Angelici, R. J. *Organometallics* **1990**, *9*, 849.

[8] Chen, J.; Angelici, R. J. *Organometallics* **1990**, *9*, 879.

[9] Chen, J.; Daniels, L. M.; Angelici, R. J. *Polyhedron* **1990**, *9*, 1883.

[10] King, R. B. *Organomet. Synth.* **1965**, *1*, 95.

[11] Sumner, C. E., Jr.; Collier, J. A.; Pettit, R. *Organometallics* **1982**, *1*, 1350.

[12] Smart, J. C.; Pinsky, B. L. *J. Am. Chem. Soc.* **1980**, *102*, 1009.

520 ($M^+ - SFe(CO)_4$), 464 ($M^+ - SFe(CO)_4 - 2CO$), 408 ($M^+ - SFe(CO)_4 - Fe(CO)_2$). Anal. Calcd for $C_{22}H_{23}O_6SIrFe_2$: C, 36.73; H, 3.22. Found: C, 36.83; H, 3.26.

Reaction of 1 with $Fe_3(CO)_{12}$ To Give 3, 6, 8, 9, and Cp*Ir(CO)$_2$ (10). To a stirred solution of **1** (60 mg, 0.136 mmol) in THF (40 mL) at room temperature was added 100 mg (0.198 mmol) of $Fe_3(CO)_{12}$. The mixture was stirred at room temperature for 24 h during which time the color of the solution turned gradually from green to dark purple. After evaporation of the solvent under vacuum, the black residue was chromatographed on Al_2O_3 (neutral) with hexane as the eluant. The purple-red band which eluted first was collected and then the orange band was eluted with hexane/CH_2Cl_2 (20:1); the third band (yellow) was eluted with hexane/CH_2Cl_2 (10:1), and finally a fourth band (dark-purple) was eluted with hexane/CH_2Cl_2/Et_2O (10:1:1). After vacuum evaporation of the solvents from the above four eluates, the residues were recrystallized from hexane or hexane/CH_2Cl_2 at −80 °C. From the first fraction, 15 mg (14%, based on **1**) of **6** as purple-red crystals were obtained (mp 143 °C dec). IR (hexane) ν_{CO}: 2008 vs, 1958 vs, 1948 s, 1720 vs, br cm^{-1}. ^1H NMR ($CDCl_3$): δ 5.59 (d, 1 H), 3.61 (d, 1 H), 2.43 (s, 3 H), 2.04 (s, 15 H), 1.85 (s, 3 H). The second fraction, a mixture of red crystalline **9** and light yellow crystalline **10**, was again chromatographed in the same manner as described above to give light yellow and orange-red fractions. The solvent was removed from each fraction in vacuo, and the residues were recrystallized from hexane at −80 °C. This yielded light yellow crystals of **10** (5 mg, 10%) and orange-red crystals of **9** (11 mg, 15%). **10**: mp 110–111 °C (lit. 145–148 °C).[13] IR (hexane) ν_{CO}: 2018 s, 1949 vs cm^{-1}.[13,14] ^1H NMR ($CDCl_3$): δ 2.17 (s). **9**: mp 178–179 °C dec. IR (hexane) ν_{CO}: 2000 vs, 1948 vs, 1842 s cm^{-1}. ^1H NMR ($CDCl_3$): δ 5.77 (s, 2 H), 2.22 (s, 6 H), 1.90 (s, 15 H). From the third fraction, 26 mg (31%) of **3** as yellow crystals were obtained (mp 162–163 °C dec). IR (hexane) ν_{CO}: 2038 vs, 1958 s, 1929 vs, br cm^{-1}. ^1H NMR ($CDCl_3$): δ 4.54 (s, 2 H), 1.94 (s, 15 H), 1.35 (s, 6 H). From the fourth fraction, 24 mg (24%) of **8** as dark blue-purple crystals were obtained (mp 140–141 °C dec). IR (CH_2Cl_2) ν_{CO}: 2040 vs, 2000 s, 1963 m, br, 1920 s, br cm^{-1}. ^1H NMR ($CDCl_3$): δ 5.68 (s, br, 1 H), 5.35 (s, br, 1 H), 2.74 (s, 3 H), 2.07 (s, 3 H), 1.79 (s, 15 H).

Reaction of 2 with $Fe_3(CO)_{12}$ To Give 3, 6, 8, 9, and 10. Similar to that described in the reaction of **1** with $Fe_3(CO)_{12}$, 60 mg (0.136 mmol) of **2** in THF (40 mL) was treated with $Fe_3(CO)_{12}$ (100 mg, 0.198 mmol) at room temperature for 20 h. The color of the solution changed gradually from green to dark green. After evaporation of the solvent under vacuum, further treatment of the resulting residue in a manner similar to that described above for the reaction of **1** with $Fe_3(CO)_{12}$ gave 20 mg (19%, based on **2**) of purple-red crystals of **6**, 7 mg (13%) of light yellow crystalline **10**, 13 mg (17%) of orange-red crystalline **9**, 16 mg (19%) of yellow crystals of **3**, and 29 mg (30%) of **8** as dark blue-purple crystals. These products were identified by comparison of their melting points and infrared and ^1H NMR spectra with those of the same compounds characterized above.

Reaction of [Cp*Ir(η^5-2,5-Me$_2$T)](BF$_4$)$_2$ (11) with (NEt$_4$)$_2$Fe$_2$(CO)$_8$ To Give 3, 7, 8, and 9. To a suspension of **11** (400 mg, 0.652 mmol) in THF (50 mL) was added 390 mg (0.654 mmol) of $(NEt_4)_2Fe_2(CO)_8$ at room temperature. The reaction mixture was stirred for 15 h during which time the color of the solution turned from brick-red to dark purple. After removal of the solvent in vacuo, the dark-purple residue was chromatographed on Al_2O_3 (neutral) with hexane as the eluant. The orange band which eluted first was collected and then a yellow band was eluted with hexane/CH_2Cl_2 (15:1); the third band (green-yellow) and fourth band (dark-purple) were eluted with hexane/CH_2Cl_2/Et_2O (10:1:1). The solvents were removed from the above four eluates in vacuo, and the residues were recrystallized from hexane/CH_2Cl_2 at −80 °C. From the first fraction, 24 mg (6.7%, based on **11**) of orange-red crystals of **9** were obtained. From the second fraction, 203 mg (51%) of yellow crystals of **3** were obtained. From the third fraction, 31 mg (6.4%) of dark green crystals of **7** were obtained. From the fourth fraction, 21 mg (4.5%) of **8** as dark blue-purple crystals were obtained. Products **3**, **7**, **8**, and **9** were identified by their melting points and IR and ^1H NMR spectra.

Reaction of 3 with $Cp_2Fe^+PF_6^-$ To Give [Cp*Ir(η^5-2,5-Me$_2$T)](PF$_6$)$_2$ (12). To a stirred solution of **3** (26 mg, 0.043 mmol) in CH_2Cl_2 (15 mL) at −10 °C was added $Cp_2Fe(PF_6)$ (29 mg, 0.088 mmol). The green yellow solution quickly turned dark orange and then light yellow. After being stirred for 0.5 to 1 h at −10 to 0 °C, the volume of the solution was reduced under vacuum to about 5 mL; to this was added 1 mL of hexane. White solid **12** precipitated, the solution was decanted, and the white product **12** was dried in vacuo; yield, 15 mg (48%, based on **3**). ^1H NMR (CD_3NO_2): δ 7.22 (s, 2 H), 2.74 (s, 6 H), 2.42 (s, 15 H). MS (FAB): *m/e* 440 (M^+). Anal. Calcd for $C_{16}H_{23}SP_2F_{12}Ir$: C, 26.34; H, 3.18. Found: C, 26.63; H, 3.27.

Reaction of 7 with $Cp_2Fe^+PF_6^-$ To Give 12. To a solution of 15 mg (0.020 mmol) of **7** in 10 mL of CH_2Cl_2 at −10 °C was added 14 mg (0.042 mmol) of $Cp_2Fe(PF_6)$. The color of the solution turned from green-yellow to deep orange. After 1 h of stirring at −10 to 0 °C, the resulting mixture was treated as described above for the reaction of **3** with $Cp_2Fe(PF_6)$ to give 6 mg (41%, based on **7**) of white solid product, **12**, which was identified by its ^1H NMR spectrum.

Reaction of 3 with CO To Give 4 and 5. Carbon monoxide gas was bubbled through a solution of 30 mg (0.049 mmol) of **3** in 40 mL of CH_2Cl_2 at room temperature for 28 h during which time the yellow solution gradually turned orange. After evaporation of the solvent in vacuo, the residue was chromatographed on Al_2O_3 (neutral) with hexane/CH_2Cl_2 (20:1) as the eluant. The yellow band which eluted first was collected and then an orange band was eluted with hexane/CH_2Cl_2/Et_2O (15:1:1). After vacuum removal of the solvents from the above two eluates, the residues were recrystallized from hexane or hexane/CH_2Cl_2 solution at −80 °C. From the first fraction, 4 mg (17%) of orange-yellow needles of **5** were obtained (mp 122 °C dec). IR (hexane) ν_{CO}: 2020 s cm^{-1}. ^1H NMR ($CDCl_3$): δ 5.73 (d, 1 H), 5.40 (d, 1 H), 2.24 (s, 3 H), 1.92 (s, 3 H), 1.85 (s, 15 H). From the second fraction, 7 mg (22%) of **4** as orange-red crystals were obtained (mp 182–184 °C dec). IR (hexane) ν_{CO}: 2035 vs, 1952 s, 1924 vs, br cm^{-1}. ^1H NMR ($CDCl_3$): δ 7.70 (d, 1 H), 7.52 (d, 1 H), 2.27 (s, 3 H), 2.03 (s, 3 H), 1.86 (s, 15 H).

Reaction of 7 with CO To Give 5. Into a 40-mL CH_2Cl_2 solution of **7** (25 mg, 0.033 mmol) at room temperature was bubbled CO gas for 15 h during which time the green solution turned orange gradually. After evaporation of the solvent, the residue was chromatographed on Al_2O_3 (neutral) with hexane/CH_2Cl_2 (20:1) as the eluant, and the yellow band was collected. The solvent was removed in vacuo and the crude product was recrystallized from hexane at −80 °C to yield 5 mg (32%) of **5** as orange-yellow needles, which were characterized by their mp, IR, and ^1H NMR spectra.

Reaction of 8 with CO To Give 9. Carbon monoxide gas was bubbled through a 30-mL CH_2Cl_2 solution of **8** (25 mg, 0.035 mmol) at room temperature for 24 h during which time the purple solution turned orange gradually. After vacuum evaporation of the solvent, the residue was chromatographed on Al_2O_3 (neutral) with hexane/CH_2Cl_2 (20:1) as the eluant. The orange eluate was collected and then evaporated to dryness under vacuum. The residue was recrystallized from hexane at −80 °C to give 3 mg (16%) of orange-red crystals of **9** (mp 178–179 °C dec). IR (hexane) ν_{CO}: 2000 vs, 1948 vs, 1842 s cm^{-1}. ^1H NMR ($CDCl_3$): δ 5.77 (s, 2 H), 2.22 (s, 6 H), 1.90 (s, 15 H).

Reaction of 3 with H_2 To Give 2. Hydrogen gas (H_2) was bubbled through a 30-mL THF solution of **3** (25 mg, 0.041 mmol) in a quartz photolysis tube while the solution was photolyzed with UV light using a 450 W, 254-nm Canrad-Hanovia mercury vapor lamp for 1 h, during which time the yellow solution turned dark-red. The solvent was removed under vacuum, and the residue was chromatographed on Al_2O_3 (neutral) with hexane as the eluant. The red eluate was collected and evaporated to dryness in vacuo. The residue was recrystallized from hexane at −80 °C to yield 11 mg (61%) of dark-red crystals of **2** (mp 147–148 °C dec). ^1H NMR ($CDCl_3$): δ 7.47 (d, 1 H), 7.34 (d, 1 H), 3.10 (s, 3 H), 2.79 (s, 3 H), 1.93 (s, 15 H).

Reaction of 7 with H_2 To Give 2. As in the reaction above, H_2 was bubbled into a 30-mL THF solution of **7** (18 mg, 0.024 mmol) in a quartz tube under UV photolysis for 1 h during which time the green solution turned dark-red. Further treatment of the resulting mixture as described above for the reaction of **3** with H_2 afforded 7 mg (66%) of dark-red crystalline **2** which was identified by its mp and ^1H NMR spectrum.

Photolysis of 3 To Give 2. A solution of **3** (20 mg, 0.033 mmol) in THF (30 mL) in a quartz photolysis tube was photolyzed with the mercury vapor lamp over a period of 12 h during which time the yellow solution turned dark-red gradually. After vacuum removal of the solvent, the residue was worked up as described for the reaction of **3** with H_2 to yield 7 mg (50%) of dark-red crystals of **2**, which was identified by its mp and ^1H NMR spectrum.

X-ray Crystal Structure Determinations of Complexes 3, 7, 8, and 9. The crystals of complexes **3**, **7**, **8** and **9** suitable for X-ray diffraction were obtained by recrystallization from hexane/CH_2Cl_2 solution at −80 °C. For each complex, a single crystal was carefully attached to the tip of a glass fiber. The X-ray diffraction intensity data were collected on an Enraf-Nonius CAD4 diffractometer at low temperature (−65 to −70 °C).

---

[13] Kang, J. W.; Moseley, K.; Maitlis, P. M. *J. Am. Chem. Soc.* **1969**, *91*, 5970.

[14] (a) Ball, R. G.; Graham, W. A. G.; Heinekey, D. M.; Hoyano, J. K.; McMaster, A. D.; Mattson, B. M.; Michel, S. T. *Inorg. Chem.* **1990**, *29*, 2023. (b) Herrmann, W. A.; Plank, J.; Bauer, Ch.; Ziegler, M. L.; Guggolz, E.; Alt, R. *Z. Anorg. Allg. Chem.* **1982**, *487*, 85.

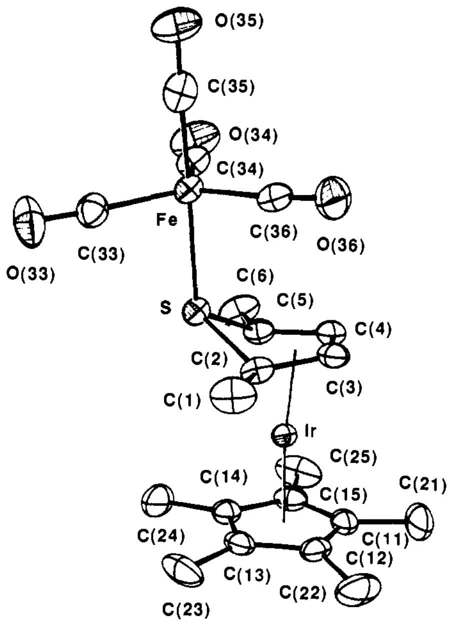

Figure 1. Structure of Cp*Ir(η^4-2,5-Me$_2$T·Fe(CO)$_4$) (3).

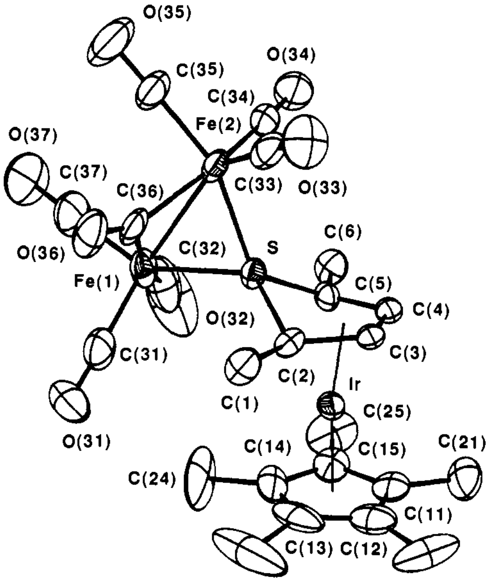

Figure 2. Structure of Cp*Ir(η^4-2,5-Me$_2$T·Fe$_2$(CO)$_7$) (7).

The cell constants were determined from a list of reflections found by an automated search routine. Relevant crystal data and details of the parameters associated with the data collection for **3**, **7**, **8**, and **9** are given in Table I. During data collection, standard reflections were measured at regular intervals to check for sample and instrument stability. No decay corrections were necessary. For each crystal, azimuthal scans of several reflections with Eulerian angle χ near 90° were used as the basis of an empirical absorption correction. The data for compound **9** were later corrected for absorption following the DIFABS[15] procedure.

The space group for each structure was unambiguously indicated by the systematic absences. The positions of the metal atoms in each structure were determined either from Patterson maps (**3**, **7**, and **8**) or from a direct-methods E-map[16] (**9**). The structures were then developed and refined in sequences of different Fourier maps and least-squares refinement. All atoms were given anisotropic temperature factors in the final cycles of refinement. For **3**, a secondary extinction coefficient was included in the refinement and converged to a value of 6.8×10^{-8} (in absolute units). Hydrogen atoms were not included in any of the models. Refinement of each structure was carried out with the CAD4-SDP package,[17] using scattering factors from the usual sources.[18]

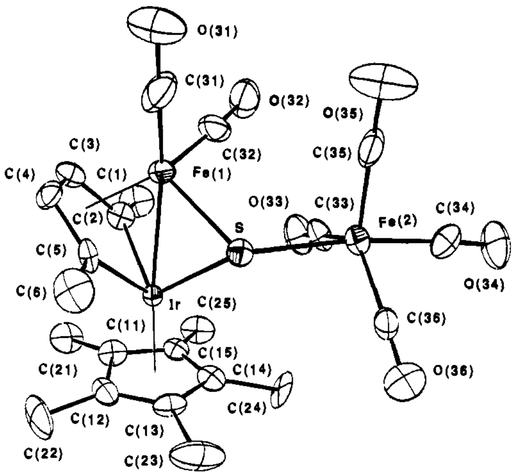

Figure 3. Structure of $\mathrm{Cp^*\overline{Ir(C(Me){=}CHCH{=}C}(Me))[\mu\text{-}SFe(CO)_4]Fe(CO)_2}$ (**8**).

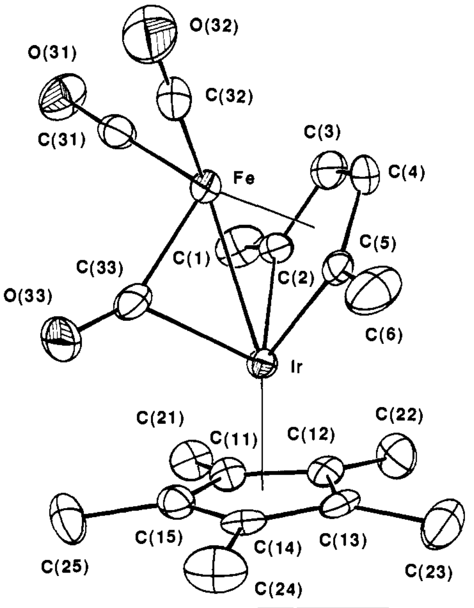

Figure 4. Structure of $\mathrm{Cp^*\overline{Ir(C(Me){=}CHCH{=}C}(Me))(\mu\text{-}CO)Fe(CO)_2}$ (**9**).

Bond lengths are listed in Tables II and III and selected bond angles are presented in Tables IV and V; ORTEP drawings with ellipsoids drawn at the 50% probability level for **3**, **7**, **8**, and **9** are given in Figures 1, 2, 3 and 4, respectively.

Results and Discussion

Reactions of 1 and 2 with Fe(CO)$_5$, Fe$_2$(CO)$_9$, and Fe$_3$(CO)$_{12}$. The **1** and **2** isomers of Cp*Ir(2,5-Me$_2$T) react at room temperature or below with Fe(CO)$_5$, Fe$_2$(CO)$_9$, and Fe$_3$(CO)$_{12}$ to give a total of eight isolated and characterized organometallic products, **3**–**10** (Scheme II); their structures are discussed below. Each iron carbonyl yields its own distribution of products but many of the same products are formed starting with different iron carbonyl reactants. Likewise, many of the same products are formed starting with either **1** or **2**. This is not surprising since **1** rearranges to the more thermodynamically stable **2** under base catalysis,[8] although we do not have direct evidence that it occurs under these reaction conditions. Reactions of either **1** or **2** with BH$_3$,[4,6,7] Cp(CO)$_2$Mo≡Mo(CO)$_2$Cp,[8] PR$_3$,[9] CO,[9] and H$_2$[9] also give the same products.

---

[15] Walker, N.; Stuart, D. *Acta Crystallogr.* **1983**, *A39*, 159.

[16] SHELXS-86, G. M. Sheldrick, Institut für Anorganische Chemie der Universität, Göttingen, F.R.G.

[17] Enraf-Nonius Structure Determination Package; Enraf-Nonius: Delft, Holland.

[18] Neutral-atom scattering factors and anomalous scattering corrections were taken from: *International Table for X-ray Crystallography*; The Kynoch Press: Birmingham, England, 1974; Vol. IV.

Table I. Crystal Data and Experimental Details for X-ray Diffraction Studies of Complexes of **3**, **7**, **8**, and **9**

	3	**7**	**8**	**9**
formula	$IrFeSO_4C_{20}H_{23}$	$IrFe_2SO_9C_{23}H_{23}$	$IrFe_2SO_6C_{22}H_{23}$	$IrFeO_3C_{19}H_{23}$
fw	607.51	747.39	719.38	547.44
space group	$P2_1/n$	$P2_1/c$	$P2_12_12_1$	$P2_1/c$
a, Å	9.096 (1)	13.319 (2)	9.6113 (6)	10.507 (2)
b, Å	14.6197 (8)	14.500 (1)	13.743 (2)	8.4858 (7)
c, Å	16.202 (2)	14.203 (2)	18.240 (2)	21.331 (6)
β, deg	101.584 (5)	111.528 (6)	$\alpha = \beta = \gamma = 90°$	103.67 (1)
V, $Å^3$	2110.5 (4)	2551.5 (5)	2409.4 (5)	1847.9 (7)
Z	4	4	4	4
d_{calc}, g/cm^3	1.912	1.946	1.983	1.968
cryst size, mm	0.20 × 0.20 × 0.11	0.26 × 0.19 × 0.12	0.12 × 0.12 × 0.14	0.56 × 0.40 × 0.20
μ(Mo Kα), cm^{-1}	70.79	64.24	67.961	79.66
data collecn instrum	Enraf-Nonius CAD4	Enraf-Nonius CAD4	Enraf-Nonius CAD4	Enraf-Nonius CAD4
radiation (monochromated in incident beam)	Mo Kα (λ = 0.71073 Å)	Mo Kα (λ = 0.71073 Å)	Mo Kα (λ = 0.71073 Å)	Mo Kα (λ = 0.71073 Å)
orientation rflns: no.; range (2θ), deg	25; 20.8–32.5	25; 21.6–32.3	25; 21.8–31.8	23; 21.8–32.0
temp, °C	−70	−70	−65	−70
scan method	θ–2θ	θ–2θ	θ–2θ	θ–2θ
data collecn range, 2θ, deg	4–50	4–50	4–50	4–50
no. of unique data				
total	3703	4468	2415	3247
with $F_o^2 > 3\sigma(F_o^2)$:	2871	3146	1984	2613
no. of params refined	245	307	289	217
transmissn factors: max/min (ψ scans)	0.9994; 0.5656	0.9985; 0.8053	0.9985; 0.8662	0.9976; 0.4936
correction factors: max, min numerical				1.325; 0.803
R^a	0.0216	0.0311	0.0336	0.0346
$R_w{}^b$	0.0308	0.0400	0.0417	0.0415
quality-of-fit indicator[c]	1.05	1.002	1.17	1.03
largest shift/esd, final cycle	<0.01	0.01	0.03	0.01
largest peak, e/$Å^3$	0.7 (1)	1.7 (2)	0.8 (2)	2.21

[a] $R = \sum||F_o| - |F_c||/\sum|F_o|$. [b] $R_w = [\sum w(|F_o| - |F_c|)^2/\sum w|F_o|^2]^{1/2}$; $w = 1/\sigma^2(|F_o|)$. [c] Quality-of-fit $= [\sum w(|F_o| - |F_c|)^2/(N_{obs} - N_{parameters})]^{1/2}$.

Table II. Bond Distances (Å)[a] for **3** and **7**

	3	**7**		**3**	**7**		**3**	**7**
Ir–C(2)	2.133 (5)	2.133 (7)	Fe(1)–C(31)		1.78 (1)	C(11)–C(12)	1.413 (8)	1.40 (1)
Ir–C(3)	2.135 (5)	2.128 (7)	Fe(1)–C(32)		1.83 (1)	C(11)–C(15)	1.427 (8)	1.43 (1)
Ir–C(4)	2.130 (6)	2.106 (7)	Fe(1)–C(36)		2.00 (1)	C(11)–C(21)	1.521 (8)	1.54 (1)
Ir–C(5)	2.123 (5)	2.163 (7)	Fe(1)–C(37)		1.77 (1)	C(12)–C(13)	1.435 (8)	1.40 (1)
Ir–C(11)	2.241 (6)	2.239 (7)	Fe(2)–S		2.186 (2)	C(12)–C(22)	1.537 (8)	1.48 (1)
Ir–C(12)	2.235 (5)	2.254 (9)	Fe(2)–C(33)		1.786 (9)	C(13)–C(14)	1.435 (8)	1.44 (2)
Ir–C(13)	2.916 (5)	2.172 (8)	Fe(2)–C(34)		1.830 (9)	C(13)–C(23)	1.512 (8)	1.54 (2)
Ir–C(14)	2.195 (5)	2.152 (8)	Fe(2)–C(35)		1.786 (8)	C(14)–C(15)	1.441 (8)	1.45 (1)
Ir–C(15)	2.193 (6)	2.177 (7)	Fe(2)–C(36)		1.929 (8)	C(14)–C(24)	1.514 (8)	1.55 (2)
Fe(1)–Fe(2)		2.599 (2)	S–C(2)	1.811 (6)	1.813 (7)	C(15)–C(25)	1.508 (9)	1.52 (1)
Fe–S	2.305 (2)		S–C(5)	1.808 (5)	1.811 (7)	C(31)–O(31)		1.15 (1)
Fe–C(33)	1.793 (6)		C(1)–C(2)	1.508 (8)	1.50 (1)	C(32)–O(32)		1.14 (1)
Fe–C(35)	1.775 (7)		C(2)–C(3)	1.464 (8)	1.45 (1)	C(33)–O(33)	1.136 (7)	1.14 (1)
Fe–C(34)	1.792 (6)		C(3)–C(4)	1.421 (8)	1.41 (1)	C(34)–O(34)	1.148 (7)	1.15 (1)
Fe–C(36)	1.778 (6)		C(4)–C(5)	1.452 (7)	1.45 (1)	C(35)–O(35)	1.156 (7)	1.144 (9)
Fe(1)–S		2.151 (2)	C(5)–C(6)	1.517 (8)	1.51 (1)	C(36)–O(36)	1.165 (7)	1.19 (1)
						C(37)–O(37)		1.14 (1)

[a] Numbers in parentheses are estimated standard deviations in the least significant digits.

In an approach to the preparation of iridium–iron–thiophene complexes which is quite different from those in Scheme II, the $Cp^*Ir(\eta^5\text{-}2,5\text{-}Me_2T)^{2+}$ (**11**) cation was reacted with the anion $Fe_2(CO)_8{}^{2-}$ (eq 2) to give a mixture of the same products that were obtained from **1** and **2** with the neutral iron carbonyls. While the mechanism of the reaction in eq 2 is not known, it is possible that it proceeds via **1** and/or **2** and iron carbonyl fragments resulting from initial electron transfer from the $Fe_2(CO)_8{}^{2-}$ to the cation. In general, all of the reactions leading to the eight products are complicated, and suggestions for their mechanisms of formation would be highly speculative. Complexes **3** and **4** are soluble in both polar and nonpolar organic solvents and are moderately air-sensitive in both the solid state and solution. Complexes **6**–**9** are soluble in polar organic solvents, are stable in air for a few hours, but are air-sensitive in solution.

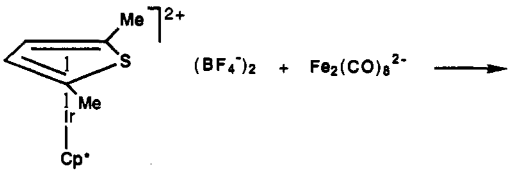

11

$$\mathbf{3} + \mathbf{7} + \mathbf{8} + \mathbf{9} \qquad (2)$$

(51) (6.4) (4.5) (6.7)

percent yields in parentheses

Of special interest are the structures of the products, which are discussed below in numerical order. Compound **3** is formed in five of the six reactions (Scheme II) in relatively high yields (19–31%). Its structure (Scheme III and Figure 1) contains a bridging 2,5-Me_2T which is η^4-coordinated through the diene portion of the thiophene to the Cp*Ir and S-bonded to the $Fe(CO)_4$. The structure is very similar to those of the BH_3 adduct, $Cp^*Ir(\eta^4,S\text{-}2,5\text{-}Me_2T\cdot BH_3)$,[4] $Cp^*Ir(\eta^4,S\text{-}\mu_3\text{-}2,5\text{-}Me_2T)$[Mo-

Table III. Bond Distances (Å)[a] for **8** and **9**

	8	**9**		**8**	**9**		**8**	**9**
Ir–Fe		2.5672 (9)	Fe(1)–C(31)	1.75 (2)		O(35)–C(35)	1.13 (2)	
Ir–Fe(1)	2.549 (2)		Fe(1)–C(32)	1.76 (2)		O(36)–C(36)	1.14 (2)	
Ir–S	2.378 (3)		Fe(2)–C(33)	1.75 (2)		C(1)–C(2)	1.52 (2)	1.53 (1)
Fe(1)–S	2.222 (4)		Fe(2)–C(34)	1.81 (2)		C(2)–C(3)	1.46 (2)	1.41 (1)
Fe(2)–S	2.298 (4)		Fe(2)–C(35)	1.81 (2)		C(3)–C(4)	1.45 (2)	1.43 (1)
Ir–C(2)	2.02 (1)	2.021 (6)	Fe(2)–C(36)	1.80 (2)		C(4)–C(5)	1.40 (2)	1.41 (1)
Ir–C(5)	2.03 (1)	2.026 (6)	Fe–C(2)		2.136 (6)	C(5)–C(6)	1.52 (2)	1.49 (1)
Ir–C(11)	2.21 (1)	2.284 (6)	Fe–C(3)		2.122 (7)	C(11)–C(12)	1.46 (2)	1.470 (8)
Ir–C(12)	2.24 (1)	2.183 (6)	Fe–C(4)		2.112 (6)	C(11)–C(15)	1.47 (2)	1.418 (9)
Ir–C(13)	2.22 (1)	2.201 (6)	Fe–C(5)		2.150 (6)	C(11)–C(21)	1.49 (2)	1.501 (9)
Ir–C(14)	2.33 (1)	2.252 (6)	Fe–C(31)		1.758 (7)	C(12)–C(13)	1.42 (2)	1.457 (9)
Ir–C(15)	2.31 (1)	2.302 (7)	Fe–C(32)		1.750 (7)	C(12)–C(22)	1.49 (2)	1.502 (9)
Ir–C(33)		2.169 (6)	Fe–C(33)		1.869 (7)	C(13)–C(14)	1.46 (2)	1.412 (9)
Fe(1)–C(2)	2.07 (1)		O(31)–C(31)	1.18 (2)	1.153 (8)	C(13)–C(23)	1.55 (2)	1.500 (9)
Fe(1)–C(3)	2.10 (2)		O(32)–C(32)	1.17 (2)	1.154 (8)	C(14)–C(15)	1.38 (2)	1.426 (9)
Fe(1)–C(4)	2.16 (1)		O(33)–C(33)	1.18 (2)	1.139 (8)	C(14)–C(24)	1.51 (2)	1.528 (9)
Fe(1)–C(5)	2.19 (1)		O(34)–C(34)	1.13 (2)		C(15)–C(25)	1.50 (2)	1.515 (9)

[a] Numbers in parentheses are estimated standard deviations in the least significant digits.

Table IV. Selected Bond Angles (deg)[a] for **3** and **7**

	3	**7**		**3**	**7**		**3**	**7**
S–Fe–C(33)	84.9 (2)		C(32)–Fe(1)–C(36)		166.7 (4)	Fe–C(34)–O(34)	174.9 (6)	
S–Fe–C(35)	173.4 (2)		C(32)–Fe(1)–C(37)		92.4 (6)	Fe–C(36)–O(36)	175.2 (5)	
S–Fe–C(34)	93.5 (2)		C(36)–Fe(1)–C(37)		86.7 (5)	S–C(2)–C(1)	117.9 (4)	118.1 (5)
S–Fe–C(36)	90.4 (2)		Fe(1)–Fe(2)–S		52.58 (6)	S–C(2)–C(3)	109.1 (4)	107.4 (5)
C(33)–Fe–C(35)	91.5 (3)		Fe(1)–Fe(2)–C(33)		137.4 (3)	C(1)–C(2)–C(3)	125.0 (5)	125.2 (7)
C(33)–Fe–C(34)	111.8 (3)		Fe(1)–Fe(2)–C(34)		108.3 (3)	C(2)–C(3)–C(4)	110.0 (5)	109.4 (7)
C(33)–Fe–C(36)	128.7 (3)		Fe(1)–Fe(2)–C(35)		107.4 (3)	C(3)–C(4)–C(5)	108.9 (5)	112.8 (6)
C(35)–Fe–C(34)	93.0 (3)		Fe(1)–Fe(2)–C(36)		49.7 (3)	S–C(5)–C(4)	110.4 (4)	106.5 (5)
C(35)–Fe–C(36)	87.5 (3)		S–Fe(2)–C(33)		99.1 (2)	S–C(5)–C(6)	117.5 (4)	120.8 (5)
C(34)–Fe–C(36)	119.5 (3)		S–Fe(2)–C(34)		96.2 (3)	C(4)–C(5)–C(6)	124.8 (5)	124.5 (6)
Fe–S–C(2)	114.3 (2)		S–Fe(2)–C(35)		159.8 (3)	Fe(1)–C(31)–O(31)		178.4 (9)
Fe–S–C(5)	116.8 (2)		S–Fe(2)–C(36)		79.2 (2)	Fe(1)–C(32)–O(32)		174 (1)
C(2)–S–C(5)	82.8 (2)	85.1 (3)	C(33)–Fe(2)–C(34)		105.6 (4)	Fe(2)–C(33)–O(33)		178.6 (8)
Fe(2)–Fe(1)–S		53.80 (6)	C(33)–Fe(2)–C(35)		96.0 (4)	Fe(2)–C(34)–O(34)		177.4 (8)
Fe(2)–Fe(1)–C(31)		135.1 (3)	C(33)–Fe(2)–C(36)		99.3 (4)	Fe(2)–C(35)–O(35)		177.3 (9)
Fe(2)–Fe(1)–C(32)		119.6 (4)	C(34)–Fe(2)–C(35)		92.4 (4)	Fe(1)–C(36)–Fe(2)		82.9 (4)
Fe(2)–Fe(1)–C(36)		47.4 (2)	C(34)–Fe(2)–C(36)		155.1 (4)	Fe(1)–C(36)–O(36)		136.5 (7)
Fe(2)–Fe(1)–C(37)		95.1 (4)	C(35)–Fe(2)–C(36)		85.2 (4)	Fe(2)–C(36)–O(36)		140.3 (8)
S–Fe(1)–C(31)		107.7 (3)	Fe(1)–S–Fe(2)		73.62 (7)	Fe(1)–C(37)–O(37)		178 (1)
S–Fe(1)–C(32)		95.4 (3)	Fe(1)–S–C(2)		123.4 (2)	C(12)–C(11)–C(15)	108.7 (5)	109.9 (8)
S–Fe(1)–C(36)		78.6 (2)	Fe(1)–S–C(5)		128.1 (2)	C(11)–C(12)–C(13)	107.9 (5)	109 (1)
S–Fe(1)–C(37)		147.3 (4)	Fe(2)–S–C(2)		123.2 (2)	C(12)–C(13)–C(14)	108.3 (5)	108.4 (9)
C(31)–Fe(1)–C(32)		101.1 (5)	Fe(2)–S–C(5)		129.6 (2)	C(13)–C(14)–C(15)	107.1 (5)	107.0 (8)
C(31)–Fe(1)–C(36)		92.1 (4)	Fe–C(33)–O(33)	177.8 (6)		C(11)–C(15)–C(14)	108.0 (5)	106.1 (9)
C(31)–Fe(1)–C(37)		101.8 (4)	Fe–C(35)–O(35)	177.9 (5)				

[a] Numbers in parentheses are estimated standard deviations in the least significant digits.

Scheme II

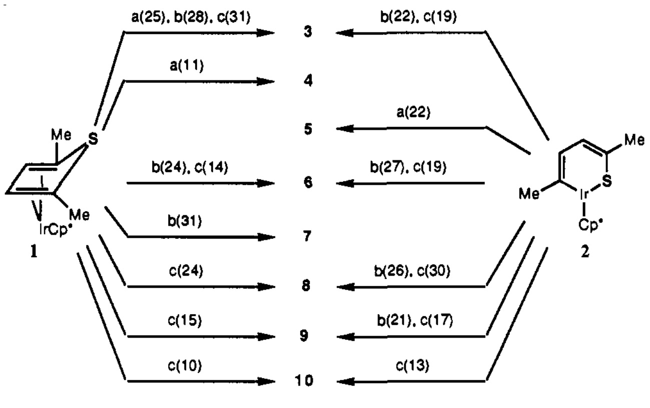

Reaction conditions: a: $Fe(CO)_5$, THF, 0-15°C, 3 h. b: $Fe_2(CO)_9$, THF, 0-15°C, 3 h. c: $Fe_3(CO)_{12}$, THF, 25°C, 20-24 h. Numbers in parentheses are percent yields. Structures of compounds **3**, **4**, **5**, **7**, **8** and **9** are given in Scheme III. Compound **10** is $Cp^*Ir(CO)_2$. Compound **6** is discussed in the text.

Scheme III

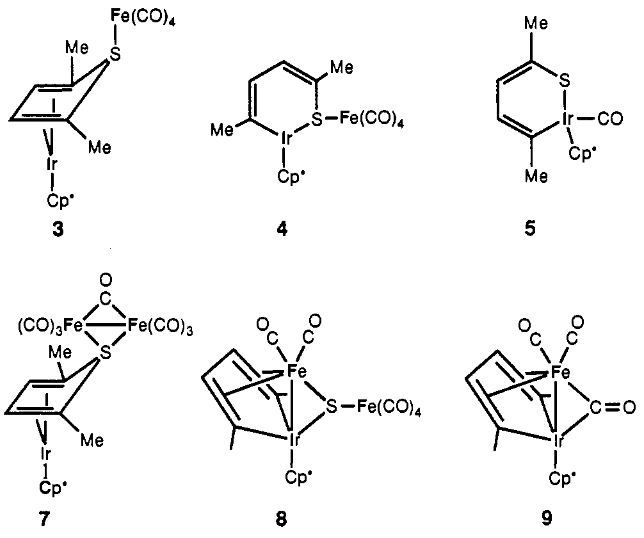

(CO)$_2$Cp]$_2$,[8] and other η^4-bonded thiophene complexes.[19] The thiophene ring is folded with a dihedral angle of 142.1 (4)° between the C(2)–C(3)–C(4)–C(5) and C(2)–S–C(5) planes, and the Ir–S distance is 2.924 (1) Å. The C(2)–S (1.811 (6) Å) and

Table V. Selected Bond Angles (deg)[a] for **8** and **9**

	8	**9**		**8**	**9**		**8**	**9**
Fe(1)–Ir–S	53.5 (1)		C(31)–Fe(1)–C(32)	93.0 (7)		C(2)–C(3)–C(4)	111 (1)	113.5 (6)
Ir–Fe(1)–S	59.3 (1)		S–Fe(1)–C(31)	104.5 (6)		C(3)–C(4)–C(5)	116 (1)	113.6 (7)
Ir–S–Fe(1)	67.2 (1)		S–Fe(1)–C(32)	100.9 (5)		C(4)–C(5)–C(6)	119 (1)	119.0 (6)
Ir–S–Fe(2)	124.0 (2)		S–Fe(2)–C(33)	91.6 (5)		Ir–C(5)–C(4)	117 (1)	117.1 (5)
Fe(1)–S–Fe(2)	118.7 (2)		S–Fe(2)–C(34)	173.7 (5)		Ir–C(5)–C(6)	124 (1)	124.0 (5)
Fe(1)–Ir–C(2)	52.3 (4)		S–Fe(2)–C(35)	88.4 (5)		Fe(1)–C(5)–C(6)	127 (1)	
Fe(1)–Ir–C(5)	55.9 (4)		S–Fe(2)–C(36)	85.8 (6)		C(12)–C(11)–C(15)	106 (1)	107.4 (6)
Fe–Ir–C(2)		53.9 (2)	C(33)–Fe(2)–C(34)	89.7 (7)		C(11)–C(12)–C(13)	108 (1)	106.6 (5)
Fe–Ir–C(5)		54.3 (2)	C(33)–Fe(2)–C(35)	113.5 (7)		C(12)–C(13)–C(14)	107 (1)	107.9 (5)
Fe–Ir–C(33)		45.5 (2)	C(33)–Fe(2)–C(36)	129.8 (8)		C(13)–C(14)–C(15)	109 (1)	109.2 (6)
S–Ir–C(2)	102.8 (4)		C(34)–Fe(2)–C(35)	96.7 (7)		C(11)–C(15)–C(14)	109 (1)	108.8 (6)
S–Ir–C(5)	76.7 (4)		C(34)–Fe(2)–C(36)	88.7 (7)		Fe(1)–C(31)–O(31)	176 (2)	
C(2)–Ir–C(5)	79.2 (6)	78.4 (3)	C(35)–Fe(2)–C(36)	116.6 (8)		Fe(1)–C(32)–O(32)	176 (1)	
C(2)–Ir–C(33)		93.0 (2)	C(31)–Fe–C(32)		91.2 (3)	Fe(2)–C(33)–O(33)	177 (2)	
C(5)–Ir–C(33)		79.8 (2)	C(31)–Fe–C(33)		99.7 (3)	Fe(2)–C(34)–O(34)	175 (1)	
Ir–Fe(1)–C(31)	150.4 (6)		C(32)–Fe–C(33)		97.9 (3)	Fe(2)–C(35)–O(35)	178 (2)	
Ir–Fe(1)–C(32)	113.5 (5)		Ir–C(2)–Fe		76.2 (2)	Fe(2)–C(36)–O(36)	177 (2)	
Ir–Fe–C(2)		49.9 (2)	Ir–C(2)–C(1)	126 (1)	124.1 (5)	Fe–C(31)–O(31)		178.7 (6)
Ir–Fe–C(5)		49.9 (2)	Ir–C(2)–C(3)	117 (1)	117.2 (5)	Fe–C(32)–O(32)		179.1 (7)
Ir–Fe–C(31)		122.2 (2)	Fe(1)–C(2)–C(1)	127 (1)		Ir–C(33)–Fe		78.6 (2)
Ir–Fe–C(32)		138.4 (2)	Fe–C(2)–C(1)		125.9 (4)	Ir–C(33)–O(33)		132.5 (5)
Ir–Fe–C(33)		55.9 (2)	C(1)–C(2)–C(3)	116 (1)	118.6 (6)	Fe–C(33)–O(33)		148.7 (5)

[a] Numbers in parentheses are estimated standard deviations in the least significant digits.

C(5)–S (1.808 (5) Å) distances are considerably longer than those (1.714 (1) Å) in free thiophene.[20] The trigonal-bipyramidal geometry around the Fe with the sulfur in an axial position is very similar to that in the thioether complex $Fe(CO)_4(1,3\text{-dithiane})$[21] and $Fe(CO)_4(SPh)^-$.[22] The ^1H NMR and IR (in the ν_{CO} region) spectra of **3** in solution are also consistent with this structure.

Compound **4** was characterized by its elemental analyses, mass spectrum which shows a parent ion and an appropriate fragmentation pattern due to CO loss, ^1H NMR spectrum which shows two H and two CH_3 groups, and IR spectrum (2035 vs, 1952 s, 1924 vs, b cm^{-1}) which is very similar to that of **3** (2038 vs, 1958 s, 1929 vs, b cm^{-1}) indicating the presence of an $Fe(CO)_4$ group. X-ray quality crystals could not be obtained, so the proposed structure (Scheme III) must be regarded as tentative.

Compound **5** was previously prepared[9] from the reaction of **1** or **2** with CO. It was assigned the structure in Scheme III based on the similarity of its ^1H NMR spectrum to those of the analogous phosphine complexes $Cp^*Ir(C,S\text{-}2,5\text{-}Me_2T)(PR_3)$ whose structures were established by X-ray diffraction studies.[9]

The composition of compound **6**, based on elemental analyses and the mass spectrum, is $Cp^*Ir(2,5\text{-}Me_2T)[Fe_2(CO)_8]$. The thiophene appears to be ring-opened as in **2** because of the presence of two H and two CH_3 signals in the ^1H NMR spectrum, and the IR spectrum exhibits a band at 1720 cm^{-1} suggesting the presence of a bridging CO group(s) between the two Fe atoms. While it is possible to propose structures which are consistent with these data, no single structure can be established without an X-ray diffraction study; unfortunately, crystals suitable for such a study were not obtained.

Compound **7** has nearly the same composition, $Cp^*Ir(2,5\text{-}Me_2T)[Fe_2(CO)_7]$, as **6**, $Cp^*Ir(2,5\text{-}Me_2T)[Fe_2(CO)_8]$, but these products clearly have different structures based on their mass, ^1H NMR, and IR spectra. An X-ray crystallographic investigation of **7** shows it to have the structure (Scheme III and Figure 2) in which the thiophene is η^4-coordinated to the Ir and the sulfur is coordinated to the two Fe atoms. As in **3**, the thiophene ring is folded with a dihedral angle between the C(2)–C(3)–C(4)–C(5) and C(2)–S–C(5) planes of 141.2 (3)° and an Ir–S distance of 2.918 (2) Å. The Fe(1)–S–Fe(2) plane intersects the C(2)–S–C(5) plane at an angle of 89.3 (2)° and the C(2)–C(3)–C(4)–C(5) plane at an angle of 93.4 (2)°. The Fe–S distances (2.151 (2) and 2.186 (2) Å) are very similar to those (2.206 (2) and 2.142 (2) Å)[23] in $Fe_3(SC_4H_8)_2(CO)_8$ which contains a triangle of Fe atoms with two edges S-bridged by tetrahydrothiophene ligands. The Fe(1)–Fe(2) distance (2.599 (2) Å) compares with 2.611 (2) Å for the bridged Fe–Fe bonds in $Fe_3(SC_4H_8)_2(CO)_8$; both are effectively single bonds. There is only one other complex in which thiophene is coordinated as in **7**, that is $Cp^*Ir(\eta^4,S\text{-}\mu_3\text{-}2,5\text{-}Me_2T)[Mo_2(CO)_4Cp_2]$ in which the Mo–Mo unit is bridged by the thiophene sulfur.[8]

In compound **8**, all of the elements of the 2,5-Me_2T ligand are present, but the sulfur is completely removed from the thiophene ring and bridges the three metal atoms. An X-ray diffraction study shows **8** to have the structure (Scheme III and Figure 3) with an iridacyclopentadiene ring η^4-bonded to the $Fe(CO)_2$ unit and the sulfur of the S–$Fe(CO)_4$ group S-bridging the Ir–Fe bond. The η^4-iridacyclopentadiene unit is characteristic of many known[24-26] dinuclear metallacyclopentadiene complexes. The geometry around the Fe in the S–$Fe(CO)_4$ group is approximately trigonal bipyramidal as it is in **3** with the sulfur in an axial positioin; the Fe(2)–S distance (2.298 (4) Å) is essentially the same as the Fe–S distance (2.305 (2) Å) in **3**. The sum of the angles around the sulfur is 309.9° which indicates that the sulfur is pyramidal.

Although it is not known how **8** forms in these reaction mixtures, one can imagine that C–S cleavage in **2**, promoted by $Fe(CO)_4$ coordination to the S, Ir, or diene, would lead to **8**. A possible pathway initiated by $Fe(CO)_4$ coordination to the Ir or S is shown in eq 3. Several other possible mechanisms could also be proposed for this reaction. Thus, although the mechanism is unknown, it is clear that iron carbonyls do promote cleavage of the C–S bond in **2**.

The structure of compound **9** (Scheme III and Figure 4) is nearly identical with that of **8** except the bridging S–$Fe(CO)_4$ group in **8** is replaced by a bridging CO in **9**. In fact, **9** is formed (16% yield) from the reaction of **8** with CO (1 atm) at room temperature for 24 h; presumably FeS or $Fe_aS_b(CO)_c$ clusters are the iron-containing products of this reaction. The geometry of

---

[19] Angelici, R. J. *Coord. Chem. Rev.* **1990**, *105*, 61.

[20] Bak, B.; Christensen, D.; Hansen-Nygaard, L.; Rastrup-Anderson, J. R. *J. Mol. Spectrosc.* **1961**, *7*, 58.

[21] Cotton, F. A.; Kolb, J. R.; Stults, B. R. *Inorg. Chim. Acta* **1975**, *15*, 239.

[22] Liaw, W.-F.; Kim, C.; Darensbourg, M. Y.; Rheingold, A. L. *J. Am. Chem. Soc.* **1989**, *111*, 3591.

[23] Cotton, F. A.; Troup, J. M. *J. Am. Chem. Soc.* **1974**, *96*, 5070.

[24] (a) Yamazaki, H.; Yasufuku, K.; Wakatsuki, Y. *Organometallics* **1983**, *2*, 726. (b) Astier, A.; Daran, J.-C.; Jeannin, Y.; Rigault, C. *J. Organomet. Chem.* **1983**, *241*, 53.

[25] (a) King, M.; Holt, E. M.; Radnia, P.; McKennis, J. S. *Organometallics* **1982**, *1*, 1718. (b) Omori, H.; Suzuki, H.; Moro-oka, Y. *Organometallics* **1989**, *8*, 1576.

[26] (a) Ogilvy, A. E.; Draganjac, M.; Rauchfuss, T. B.; Wilson, S. R. *Organometallics* **1988**, *7*, 1171 and references therein. (b) Hübener, P.; Weiss, E. *J. Organomet. Chem.* **1977**, *129*, 105.

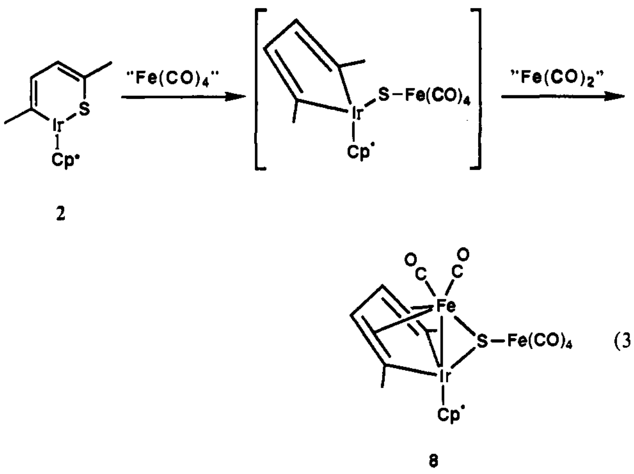

(3)

the iridacyclopentadiene portion of **9** is typical of metallacyclopentadiene complexes,[24-26] some of which have been prepared from iron carbonyls and thiophenes.[26] Analogous Co[24] and Rh[26a,27] complexes are known and have structure A. This structure differs from that of **9** in that the Fe rather than Co or Rh is part of the

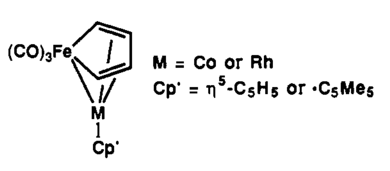

A

metallacyclopentadiene ring, and also there is a bridging CO in **9**. It is particularly striking that the A complex with M = Rh, Cp′ = C_5Me_5, and four methyl groups on the diene is obtained from the reaction[27] of Cp*Rh(η^4-Me_4T), Me_4T = tetramethylthiophene, with $Fe_3(CO)_{12}$ in toluene at 110 °C for 18 h. Except for the more strenuous conditions, this reaction is very similar to that of **1** with $Fe_3(CO)_{12}$ (Scheme II) which gives **9**. Whether it is the different reaction conditions or the different metal (Rh vs Ir) that controls which metal is incorporated into the metallacyclopentadiene ring is not known. However, it seems likely that the observed structures are thermodynamically the most stable because there is probably a facile pathway for exchange of the metal sites, as has been established in the dinuclear metallacyclopentadiene complex ($CpCoC_4H_4$)CoCp.[28]

Reactions of 3 and 7. To examine the possibility that the Cp*Ir(CO)$_2$ (**10**) product in Scheme II was formed by CO displacement of the η^4-diene from **3** or **7**, we reacted **3** and **7** with CO (1 atm) at room temperature (eqs 4 and 5). In the reaction

$$\mathbf{3} + \mathrm{CO} \xrightarrow[28\ \mathrm{h}]{25\ ^\circ\mathrm{C},\ \mathrm{CH_2Cl_2}} \mathbf{4} + \mathbf{5} \qquad (4)$$

$$\mathbf{7} + \mathrm{CO} \xrightarrow[15\ \mathrm{h}]{25\ ^\circ\mathrm{C},\ \mathrm{CH_2Cl_2}} \mathbf{5} \qquad (5)$$

of **3**, only its isomer **4** (22%) and **5** (17%) in which there is no iron were produced. The reaction of **7** with CO yielded only **5**, presumably resulting from CO displacement of the iron carbonyl from the sulfur; the resulting Cp*Ir(η^4-2,5-Me_2T) (**1**) is known[9] to react with CO to give **5**. Thus, neither of the reactions in eq 4 or eq 5 are the source of **10**.

Seeking reactions of H_2 which might be of interest for hydrodesulfurization, complexes **3** and **7** were reacted with H_2 (1 atm). Neither complex in CH_2Cl_2 or THF reacted at room temperature over a period of 12–24 h. Under ultraviolet photolysis both complexes gave **2** (61–66% yield) within only 1 h; even in the absence of H_2, photolysis of **3** yielded **2**. These reactions presumably involve initial photolytic dissociation of **1** from the starting complexes. Under photolysis, **1** is then probably isomerized to **2**, since this isomerization does occur under these conditions.

Both **3** and **7** are quickly oxidized (eq 6) by Cp_2Fe^+ to give Cp*Ir(η^5-2,5-Me_2T)$^{2+}$ in 48 and 41% yields, respectively. Although the fate of the iron carbonyl is not known, the oxidation presumably occurs at the Ir since it is more electron-rich than the iron carbonyl unit.

(6)

Relevance to Hydrodesulfurization (HDS). The goal of these studies was to explore the possibility that reactions of **1** and **2** would suggest new possible mechanisms for thiophene desulfurization on heterogeneous HDS catalysts. We had previously demonstrated (eq 1)[4] that the η^4-thiophene ring in Cp*Ir(η^4-2,5-Me_2T) (**1**) undergoes base-catalyzed C–S cleavage with insertion of Ir into the ring to give Cp*Ir(*C,S*-2,5-Me_2T) (**2**). We now find that the remaining C–S bond in **2** is cleaved upon reaction with iron carbonyls to form products **8** and **9**. Thus, a second metal does, in some fashion, promote this cleavage and also participates in stabilizing the resulting fragments in **8**. One possible mechanism for the conversion of **2** to **8** is suggested in eq 3. These C–S bond cleavage reactions, if they were to occur at metal centers on an HDS catalyst, provide a reasonable mechanism for thiophene HDS.

Scheme IV. C–S Cleavage Mechanism for Thiophene HDS

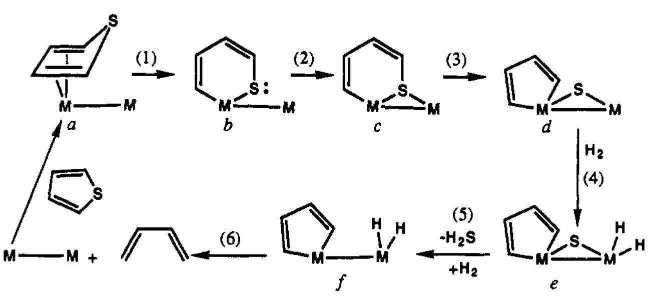

Such a mechanism is shown in Scheme IV. Although the most common mode[3,19] of thiophene coordination in transition-metal complexes is η^5 via the entire π-system of the ring, it is possible that for either electronic or steric reasons η^4-coordination occurs at the active sites on the catalyst. This mode of adsorption could activate the thiophene to undergo C–S cleavage (step 1 in Scheme IV) while incorporating the metal into the 6-membered ring in intermediate *b*, as occurs in the conversion of **1** to **2** (eq 1).[4] This latter conversion is base-catalyzed but details of the mechanism are not known; on an HDS catalyst, it could either be promoted by a basic species, e.g., O^{2-} or S^{2-}, or occur spontaneously.[29] Cleavage of the second C–S bond is proposed to occur in steps 2 and 3 which involve initial coordination of the sulfur to an adjacent metal site (*c*) followed by C–S cleavage with formation of the metallacyclopentadiene (*d*) in step 3. Steps 2 and 3 are very similar to the overall reaction of **2** with iron carbonyls to give **8** (Scheme II, eq 3); however, in the case of **8**, the bridging sulfide is coordinated to an $Fe(CO)_4$ group and the diene portion of the iridacyclopentadiene is coordinated to another iron; it is possible that the diene in *d* would also be coordinated to an adjacent metal site. It is noteworthy that others[30] have obtained evidence for a

---

[27] Ogilvy, A. E.; Skaugset, A. E.; Rauchfuss, T. B. *Organometallics* **1989**, *8*, 2739.

[28] Rosenblum, M.; North, B.; Wells, D.; Giering, W. P. *J. Am. Chem. Soc.* **1972**, *94*, 1239.

[29] Ring-opened thiophenes of type *b* (Scheme IV), but which are stabilized by coordination of the ring to another Fe, have been obtained from reactions of iron carbonyls with thiophenes.[26]

metallacyclopentadiene of the type in *d* from the decomposition of thiophene on Pt(111). Steps 1, 2, and 3 constitute a new mechanism for the cleavage of both C–S bonds prior to any hydrogenation of the thiophene ring. Although other mechanisms for thiophene HDS involving C–S cleavage prior to hydrogenation have been proposed,[31] none is based on reactions which are known to occur on metal centers.

Following the formation of intermediate *d* in Scheme IV, the C_4 ring and sulfide could be removed from the catalyst by reaction with adsorbed hydrogen to give butadiene and H_2S. The mechanism in Scheme IV shows the adsorbed hydrogen in the form of surface hydrides M–H; however, it is also possible that the hydrogen is present in –SH groups; there is ample evidence to suggest that –SH ligands may be a good source of hydrogen atoms.[32] To our knowledge, there are no examples of H_2S elimination from M(H)(SH) or $M(H)_2(S)$ complexes which would support step 5; however, there are several reports of the reverse reaction, i.e., H_2S addition to mononuclear[33] or polynuclear[34] metal complexes to give products with H, SH, or S ligands. Thus, the mechanism in Scheme IV represents a reasonable process for thiophene desulfurization.

Unlike our previous mechanism (Scheme I), that in Scheme IV does not involve initial hydrogenation of the thiophene ring and therefore, represents a fundamentally different type of thiophene HDS mechanism. Results of reactor studies have been interpreted[32] to suggest that there are two HDS processes occurring at different sites; one begins by initial hydrogenation of thiophene while the other begins with C–S bond cleavage. Schemes I and IV represent reasonable mechanisms for these processes; both are based on known reactivity of thiophene in its organometallic complexes. It remains to be determined whether or not similar processes occur on HDS catalyst surfaces.

Acknowledgment. We appreciate the loan of $IrCl_3$ from Johnson Matthey, Inc.

Supplementary Material Available: Tables of positional parameters, additional bond angles, torsion angles, displacement parameters, and least-squares planes for complexes **3**, **7**, **8**, and **9** (39 pages); listing of calculated and observed structure factors (55 pages). Ordering information is given on any current masthead page.

---

(30) (a) Stohr, J.; Gland, J.; Kollin, E. B.; Koestner, R. J.; Johnson, A. L.; Muetterties, E. L.; Sette, F. *Phys. Rev. Lett.* **1984**, *53*, 2161. (b) Lang, J. F.; Masel, R. I. *Surf. Sci.* **1987**, *183*, 44. (c) Patterson, C. H.; Mundenar, P. Y.; Timbrell, A. J.; Gellman, A. J.; Lambert, R. M. *Surf. Sci.* **1989**, *208*, 93.

(31) Prins, R.; DeBeer, V. H. J.; Somorjai, G. A. *Catal. Rev.-Sci. Eng.* **1989**, *31*, 1.

(32) Rakowski Dubois, M. *Chem. Rev.* **1989**, *89*, 1.

(33) (a) Lee, C.-L.; Chisholm, J.; James, B. R.; Nelson, D. A.; Lilga, M. A. *Inorg. Chim. Acta* **1986**, *121*, L7. (b) Osakada, K.; Yamamoto, T.; Yamamoto, A. *Inorg. Chim. Acta* **1985**, *105*, L9. (c) Bottomley, F.; Drummond, D. F.; Egharevba, G. O.; White, P. S. *Organometallics* **1986**, *5*, 1620.

(34) (a) Bensenyei, G.; Lee, C.-L.; Gulinski, J.; Rettig, S. J.; James, B. R.; Nelson, D. A.; Lilga, M. A. *Inorg. Chem.* **1987**, *26*, 3622. (b) Jennings, M. C.; Payne, N. C.; Puddephatt, R. J. *Inorg. Chem.* **1987**, *26*, 3776. (c) Antonelli, D. M.; Cowie, M. *Inorg. Chem.* **1990**, *29*, 3339.

Stable Polyradicals with High-Spin Ground States. 1. Synthesis, Separation, and Magnetic Characterization of the Stereoisomers of 2,4,5,6-Tetrachloro-$\alpha,\alpha,\alpha',\alpha'$-tetrakis(pentachlorophenyl)-*m*-xylylene Biradical[1]

Jaume Veciana,*[†] Concepció Rovira,[†] Maria I. Crespo,[†] Olga Armet,[†] Victor M. Domingo,[†] and Fernando Palacio[‡]

Contribution from the Institut de Ciència de Materials de Barcelona-CID, CSIC, C. Jordi Girona 18-26, 08034 Barcelona, Spain, and the Instituto de Ciencia de Materiales de Aragón, CSIC—Universidad de Zaragoza, 50009 Zaragoza, Spain. *Received January 3, 1990. Revised Manuscript Received October 3, 1990*

Abstract: Biradical **3** and its corresponding monoradical **6** have been synthesized and isolated as stable solids at ambient conditions. Biradical **3** exists in three stereoisomeric forms due to restricted correlated rotation of the aryl groups. It has been obtained as a 60:40 equilibrated mixture of the *meso* form (C_s symmetry) and the enantiomeric *dl* pair (C_2 symmetry) which have been unambiguously identified by ESR spectroscopy. Recrystallization of the diastereoisomeric mixture afforded the pure *meso* form. Both diastereoisomers have been separated by HPLC chromatography and their interconversion rates have been measured at different temperatures. The diastereoisomerization barrier [$\Delta G^{\ddagger}_{298K}$ (*meso* → *d*(or *l*)) = 98 kJ mol^{-1}] is comparable to that of related monoradicals with similar steric hindrances. Intense triplet ESR signals were obtained in rigid media, being $|D/hc| = 0.0152$ and $|E/hc| = 0.0051$ cm^{-1} for the *meso* and $|D/hc| = 0.0085$ and $|E/hc| \leq 0.003$ cm^{-1} for the *dl* isomer. The observed zero-field splitting parameters for both stereoisomers are consistent with their symmetries. Curie plot studies on ESR signals are in agreement with triplet ground states for both diastereoisomers irrespective of their symmetries. Magnetic susceptibility and magnetization measurements of the diastereoisomers in solid state show quasi-ideal $S = 1$ paramagnetic behavior down to 4.2 K. For one representative case, the results presented here validate the current theories for the prediction of ground-state multiplicities in nondisjoint AH, regardless of the lack of planarity and changes in the symmetries.

Current research on magnetic organic materials aims toward the design and preparation of organic ferromagnets. Although no such substance has been so far found, several strategies and theoretical models have been described for designing this type of material.[2] One of these strategies consists of obtaining molecules possessing a spin multiplicity as high as possible and having them

---

[†] Institut de Ciència de Materials de Barcelona—CID.

[‡] Instituto de Ciencia de Materiales de Aragón.

(1) A brief report of this work was presented at the Symposium on Ferromagnetic and High-Spin Molecular Based Materials; 197th National Meeting of the American Chemical Society, Dallas, TX, April 9–14, 1989. Veciana, J.; Rovira, C.; Armet, O.; Domingo, V. M.; Crespo, M. I.; Palacio, F. *Mol. Cryst. Liq. Cryst.* **1989**, *176*, 77–84.